MARINER-9-BASED SIMULATION OF RADIATIVE CONVECTIVE TEMPERATURE CHANGES IN THE MARTIAN DUST-LADEN ATMOSPHERE-SOIL SYSTEM

William P. Dannevik and Albert J. Pallmann

Division of Atmospheric Science

Saint Louis University, Missouri 63103

January 1974

Abstract

A numerical simulation of radiative, conductive, and convective heat transfer of the Martian dust-laden atmosphere-soil system is presented with particular emphasis given to heating/cooling in regions of sharp variation in temperature or absorption and its resultant impact on outgoing planetary spectral radiance, as measured by the Mariner 9 IRIS. Thermal coupling between the ground and atmospheric subsystems is modeled by the total heat flux balance at the interface. In the simulation procedure, local thermodynamic equilibrium (LTE) is assumed, and a combined strong-weak line transmission function permits short- and long-range exchanges of energy from the surface toward space. Direct absorption of insolation in the near-IR bands by both silicate dust and CO_2 is incorporated. The thermal coupling appears as a boundary-initial value problem which has been solved through forward-time integration in 15-minute steps. The input data base stems from various experiments flown on Mariner 9. Results of interest are: (1) atmospheric counter-radiation is increased by more than 50% in the presence of dust, (2) tropospheric convective mixing is confined to the lowest 5 km, (3) quasi-isothermal stratification results in the upper part of the dust layer during the period of intense solar heating, (4) a highly effective radiation-convection layer exists at the top of the dust stratum with a diurnal temperature variation of 40 K.

Zusammenfassung

Eine numerische Simulation des Wärmetransports durch Strahlung, Wärmeleitung und Konvektion in dem staubgeladenen Atmosphäre-Boden System des Planeten Mars wird vorgelegt, die insbesondere Erwärmung und Abkühlung in den Bereichen scharfer Änderung der Temperatur oder Absorption berücksichtigt mit dem sich daraus ergebenden Einfluss auf die aufwärts gerichtete, planetarische, spectrale Radianz, wie sie durch Mariner 9 IRIS gemessen wurde. Die thermische Koppelung zwischen dem Boden und dem atmospharischen System ist modellmässig gegeben durch die Bedingung der Kontinuität des totalen Wärmeflusses an der Zwischenfläche. Der Modellierungsvorgang sieht lokales thermodynamisches Gleichgevicht (LTE) vor; eine kombinierte Transmissionsfunktion für starke und schwache Absorptionslinien erlaubt Energieaustausch über kurze und weite Distanzen vom Boden bis zu grossen Höhen. Ausserdem ist direkte Absorption der Sonnenstrahlung im nahen Infrarot einbezogen für Silikatstaub und Kohlendioxyd. Die thermische Koppelung stellt sich als Grenz-Anfangswert-Problem dar, das durch Vorwärtsintegration in 15-Minuten Intervallen gelöst worden ist. Die Eingabedaten stammen von verschiedenen Experimenten, die mit Mariner 9 geflogen wurden. Ergebnisse von Interesse sind: (1) atmosphärische Gegenstrahlung nimmt um mehr als 50% zu, wenn Staub gegenwärtig ist; (2) troposphärisch-konvektive Mischungsvorgänge sind auf die untersten 5 km beschränkt; (3) quasi-isothermische Schichtung ergibt sich im oberen Teil der Staubschicht während der Zeitspanne intensiver solarer Erwärmung; (4) eine Schicht hochwirksamer Strahlungsdivergenz und Konvektion existiert an der Obergrenze der Staubschicht, die eine ganztägige Temperatur-schwankung von etwa 40°K aufweist.

1. Introduction

The global extent of sand-like dry soil material on Mars permits the surface temperature field to respond rapidly to changes of largely-unattenuated insolation, with the mid-latitudinal diurnal variation being ~ 70K. In addition, the predominance of CO_2 and relative tenuity of the Martian atmosphere result in a large radiative response capability; therefore, a significant diurnal thermal boundary layer is induced even if convection were absent. Analysis of radiative relaxation times for Mars (Goody and Belton, 1967) indicates a characteristic depth of 1.6 km for the diurnal temperature wave. The latter study also shows that molecular conduction may be an important transfer mechanism for thermal perturbations of spatial scale $< O(10m)$.

The purpose of this note is to present some first findings of a numerical modeling developed to (1) investigate the thermal coupling of the Martian atmospheric and soil subsystems, and the resultant diurnal temperature variation in the lowest scale-heights of the atmosphere and (2) develop some criteria for the interpretation, under the condition of atmospheric dust loading, of Mariner 9 IRIS inverted data.

The design of the numerical model departs in several essential ways from that employed by Gierasch and Goody (1967, 1968). In the latter model, a "trapozoidal rule" was used to approximate the exchange integral for planetary radiative

heating, correctly accounting for the boundary terms while representing the contribution from various atmospheric source layers with emission terms evaluated at two discrete points which are sometimes far apart. This approximation emphasizes the long-range exchange but eliminates the effects of short-path, strong-line radiative transfers. On the other hand, a strong-line approximation to the transmission function was used throughout. A bulk transmission for the 15μ CO_2 band was utilized, without temperature dependence in either the integrated line intensity or Lorentz half-width. As Gierasch and Goody have pointed out, the resulting model is not effective for phenomena involving small length scales, such as radiative heating/cooling near a region of sharp variation in temperature or absorption.

It is precisely the latter phenomena which are of greatest interest in the present study. We are especially concerned with (1) the diurnal history of thermal structure near the soil-atmospheric interface and the extremities of a suspended dust layer, and with (2) the impact of relatively small-scale temperature variation on the outgoing planetary spectral radiance such as would be measured by the Mariner 9 Infrared Interferometer Spectrometer (IRIS). The model described in the present paper is most effective for study of variations in heat exchange and thermal structure in the free-atmospheric layers above the daytime convective boundary layer, and in the near-surface regions when the boundary layer is

stably-stratified. Expansion of the model to account for a time-dependent free-convective boundary layer will be described in a forthcoming article. In the present paper, we report these findings which are expected to be little affected by the inclusion of the convective boundary layer.

2. Simulation Procedure

The atmospheric model adopted is that of a 100% CO_2 atmosphere in local thermodynamic equilibrium (LTE), with plane-parallel stratification and negligible Doppler broadening (Pallmann, 1968; Pallmann and Dannevik, 1972). The lower solid surface is assumed horizontal and of silicate composition. The effect on heat exchange of dust suspended in the lowest scale heights is incorporated by considering the increase of effective radiative path length induced by multiple scattering and the additional direct absorption by the dust particulates themselves.

From dynamical scaling considerations and radiative relaxation time estimates, Gierasch and Goody (1968) have inferred that in the first approximation, temperature change due to advection by the mean wind field may be neglected compared with that due to radiative, molecular-conductive, and turbulent-convective transport. Thus, the atmospheric response to surface temperature variation may be investigated without calculating the large-scale horizontal motion field (Gierasch, 1971).

Details of the coupling between Martian soil and atmospheric temperature variation depend crucially on the structure of the CO_2 absorption bands. Since most of the 15μ -band absorbs strongly even under the reduced surface pressure conditions of Mars ($\sim$ 6 mb), a portion of the coupling will occur through the near-surface layers. Strong-line radiative transfer will approximate a diffusion process in these layers, augmented by the conductive-convective heat transports induced by large temperature gradients. On the other hand, spectral "gappiness" and weak-line transmission, each enhanced by atmospheric tenuity, will permit some long-range exchange of energy from the surface to several scale heights and toward space (Drayson, 1972). This longer-range exchange approximates a Newtonian cooling (Kuo, 1968; Schlichting, 1960).

Several factors serve to complicate the integrated radiative-conductive-convective exchange process. Among these are direct absorption of insolation in the near-IR CO_2 bands, the presence of spectral lines of intermediate intensity, substantial variations in gas-kinetic properties along the radiative path length, and the presence of dust-aerosol in the troposphere. One of the effects of the latter is to increase gaseous absorption, since multiple scattering results in a longer effective radiative path length. In addition, the dust particulates may directly absorb both solar and planetary radiation.

At the soil-atmosphere interface, a discontinuity in physico-optical properties occurs, although on a physical basis we may still expect the resultant net flux of heat to remain continuous across the interface. The net heat flux includes contributions from short- and long-wave radiation and molecular-conductive fluxes in the soil and atmosphere. An additional physical constraint is a tendency toward a matching of temperature determined by molecular conduction in the soil sub-system and the radiative-conductive temperature in the atmospheric layers. This tendency is complementary to the LTE condition.

In devising the simulation procedure, we have incorporated to some extent each of the above mentioned physical processes into a computer model, except for turbulent-convective heat transport. To accommodate the latter, the computer-generated temperature profiles have been submitted to a convective adjustment in the appropriate atmospheric region above the constant flux layer. The depth of this convective region has been determined on the basis of complete adiabatic mixing.

Thermal coupling of the soil and atmosphere may be studied as a boundary-initial-value problem through a forward time integration of the applicable heating rate equation. In our context, this relation takes the form

$$\rho c\frac{\partial T}{\partial t}(x,t) = \frac{\partial}{\partial x}(k\frac{\partial T}{\partial x}) + 2\pi\int_{o}^{\infty}\rho\kappa_{\nu}\Big\{\mu S_{\nu}(0)\exp(-\int_{o}^{x}\rho\kappa_{\nu}ds\mu^{-1}) +$$

$$G_{\nu}(t)\exp(-b\int_{x}^{x_s}\rho\kappa_{\nu}ds) + \int_{o}^{x}B_{\nu}(\xi,t)\frac{\partial}{\partial\xi}\Big[\exp(-b\int_{\xi}^{x}\rho\kappa_{\nu}ds)\Big]d\xi$$

$$+\int_{x}^{x_s}B_{\nu}(\xi,t)\frac{\partial}{\partial\xi}\Big[\exp(-b\int_{x}^{\xi}\rho\kappa_{\nu}ds)\Big]d\xi - 2B_{\nu}(x,t)\Big\}d\nu,$$

$$0<x<x_s,\ t>0 \qquad (1a)$$

$$\rho_s c_s\frac{\partial T_s}{\partial t}(x,t) = \frac{\partial}{\partial x}(k_s\frac{\partial T_s}{\partial x}),\ x_s<x<x_d,\ t>0 \qquad (1b)$$

where:

T,ρ,c,k	temperature, density, specific heat, and thermal conductivity in the atmospheric (no subscript) and soil subsystem (subscript "s")
x,ξ	depth, measured from top of atmosphere
x_s	soil-atmosphere interface level
x_d	lowest level considered in soil subsystem
$\arccos(\mu)$	solar zenith angle at time t
κ_{ν}	mass absorption coefficient at frequency ν
B_{ν}	specific intensity of blackbody emission
G_{ν}	upwardly-directed specific intensity at the interface level due to thermal emission or diffuse reflection of solar irradiation
S_{ν}	spectral solar radiation at the actual Sun-Mars distance
b	diffusivity factor.

The functions T, ρ, κ_ν, and B_ν depend on depth and time, while μ and G_ν depend on time.

Continuity of the total net flux of heat at the interface requires that

$$F_n(x_s-0,t) - F_n(x_s+0,t) = 0. \qquad (2)$$

In terms of the relevant component fluxes, this relation represents an internal boundary condition for the level x_s:

$$2\pi\int_0^\infty\int_0^{x_s-0} B_\nu(\xi,t)\exp\left(-b\int_0^\xi \rho\kappa_\nu ds\right)\rho\kappa_\nu d\xi d\nu - \sigma\varepsilon T_s^4(x_s-0,t) +$$

$$2\pi\int_0^\infty (1-\alpha_s)\mu S_\nu(0)\exp\left(-\int_0^{x_s-0}\rho\kappa_\nu ds\mu^{-1}\right)d\nu - k\frac{\partial T}{\partial x} + k_s\frac{\partial T_s}{\partial x} = 0,$$

$$x = x_s,\ t \geq 0. \qquad (3a)$$

Here, σ, ε, and α_s represent the Stefan-Boltzmann constant, IR-emissivity, and surface albedo. Matching of temperature at the interface is expressed as

$$T(x_s-0,t) = T_s(x_s+0,t). \qquad (3b)$$

In (1) and (3a), it is assumed that no phase changes of CO_2 occur.

The upper boundary condition at an elevation of 50 km (x=0) is set as vanishing incoming thermal radiation and constant temperature. Finally, the lower boundary condition at $x=x_d$ is that of constant temperature.

A quasi-random model using the band parameters of Prabhakara and Hogan (1965) has been chosen for the transmission functions appearing in (1a) and (3a), and a weak- or strong-line limit is employed, based on the magnitude of radiative path length pertinent to a given spectral and geometric interval. Frequency integration is performed over 62 intervals embracing the 1-6μ and 12-18μ vibration-rotation bands. In those atmospheric strata assumed dust-laden, the gaseous transmission is reduced by a factor $\exp(-\beta_d \Delta x)$, where β_d is an "effective absorption" coefficient due to dust, and Δx is the thickness of the layer. The cumulative fraction of irradiated solar energy flux which is contained in the modeled CO_2 near-IR bands constitutes about 9% of the total insolation. With $\beta_d = 0.1\,\mathrm{km}^{-1}$ and the total depth of the dust layer being 30 km, the model thus produces approximately an additional 9%-attenuation of the vertical solar radiation, which is converted into heat within the dust layer. Gierasch and Goody (1972) utilized a 10%-attenuation under grey absorption.

To accomodate the inhomogeneity of temperature, pressure, and density, the transmission function for an extended path is approximated by a product of transmission functions taken over a number of intervening sub-layers, within each of which the gas-kinetic properties do not vary appreciably. The dependence of line intensity and Lorentz half-width on temperature and effective pressure is included in the calculation of individual layer transmission functions.

The integrals over depth in (1a) and (3a) must be evaluated by numerical quadrature. In view of spectral gappiness in the absorption spectrum and inclusion of molecular thermal conduction in the heating-rate equation, we anticipate a relatively complex structure of the vertical temperature profile in the boundary layer. A 52-point quadrature formula has been adopted, with 7 points distributed in the lowest km, and generally a 1 km spacing in the region between 1 and 50 km. This resolution restricts the relative variation of Planck function to $\lesssim$ 3% in a given layer, under representative conditions. The same spacing is used to construct finite difference approximations to the spatial derivatives in (1a), while a 2-cm increment is used in the soil sub-system.

From the estimates of Goody and Belton (1967), the characteristic time for relaxation of thermal perturbations having scales of the order of several meters is in the range of 10^3 sec for the Martian troposphere. On these physical grounds, we may infer that a computational time increment of similar size is required to adequately resolve in time the propagation of temperature waves in the near-surface region. A 15-minute time step was used for all calculations discussed in this note.

The computational procedure begins with calculation of transmission functions, solar spectral irradiance, and atmospheric spectral emission corresponding to the initial time and temperature distribution. These quantities are then combined to form the total (radiative + conductive) heating/cooling function represented on the right-hand-side of (1a). Flux components in (3a) are then computed, and this relation and (1b) are solved for the soil temperature field for the end of the first timestep. Then, (1a) is solved for the new atmospheric temperature field, using (3b) as the lower boundary condition. The new soil-atmosphere temperature profile is then used as input for the next timestep, and new solar spectral irradiances are calculated for the advanced local time. In this manner,

the procedure continues through the total interval of time desired for the simulation.

Numerical values for physico-optical properties of the simulated soil material were derived through an independent parametric study, in which the JPL (1968) thermal inertia values were adjusted until calculated diurnal surface temperature variation matched that suggested by recent Mariner radiometric scans. Raw spectral solar radiation data are those reported by Robinson (1965), adjusted to the Martian season and latitude relevant to a given simulation.

The initial atmospheric sounding data are derived from preliminary Mariner 9 IRIS inversion profiles kindly furnished by Drs. Hanel and Pearl of the Goddard Space Flight Center, and correspond to 1900 local Martian time (LMT), latitude 38°S, and solar declination -23° (Southern hemisphere summer).

3. Some results and preliminary interpretation

Numerical output of the model for each timestep basically consists of the thermal structure between the levels of 60 cm soil depth and 50 km atmospheric height, radiative fluxes of solar, atmospheric, and surface origin in each of 62 wave number intervals between 1.29 and 18.02μ, and the

radiative and molecular-conductive heating/cooling rates at each computational level. Results presented here are based on two simulations, each representing an interval of 24 Martian hours. The first case, designated "dust-free", utilizes as initial data the Mariner 9 IRIS inversion profile (Hanel et al., 1972) mentioned previously, with a starting time of 1900 LMT. The second case uses an identical initial sounding and starting time, but includes a simulated ground-based dust layer of 30 km thickness; this case will be termed "dust-laden".

Since over the night-time hours the radiative conductive model is thermally dissipative, minor inconsistencies between the arbitrary subsoil and surface temperature and the atmospheric sounding tend to dissappear with time, so that by sunrise, the entire temperature profile is thermally "initialized".

Fig. 1 depicts modeled atmospheric soundings for 0500 and 1600 LMT for each simulation. With regard to the dust-free case, three basic regimes are evident. The lowest regime, from the surface to about 5 km, includes those atmospheric strata dominated by strong-line, short-path, diffusion-like radiative and convective exchange associated with soil surface temperature variation. The regime between

5 and 31 km is "in communication" with surface temperature variation primarily through weak-line exchange, but also undergoes direct solar heating and weak-line losses to outer space. The regime above 31 km is dominated by the upper boundary conditions, i.e., direct solar heating and emission to outer space, and is affected little by soil surface temperature variation, which lags solar forcing by roughly 4 hours.

Soundings from the dust-laden case exhibit essential differences from those of the dust-free simulation primarily in the middle regime (5-31 km; placement of the top of the simulated dust layer at about the same level as the upper bound of the middle regime for the dust-free case is coincidental). Over the daylight hours, this region approaches an isothermal stratification, in agreement with recent Mariner 9 findings showing a tendency towards this structure in the dust-laden mission phases. The top of the dust layer acts as an "effective radiation surface", similar to its radiative response to the solid soil surface. Diurnal temperature variation at the top of the dust layer is nearly 50% of the amplitude of surface temperature variation. Thus, the upper regime (above $\sim$ 31 km) reacts to this effective radiation table in the same way that the lowest regime acts to surface temperature variation in the dust-free case. In

particular, the radiation table induces a statically unstable stratification at the top of the dust layer in the afternoon hours. The lapse rate of the layer was subsequently adjusted to the adiabatic value to reflect convective mixing.

The Mariner 9 IRIS profile was derived by inverting the IRIS radiance measurements obtained during a dust-laden mission phase, to generate a temperature profile assuming a dust-free atmosphere. This initial temperature profile approximates a smoothed version of the modeled 1600 LMT output for the dust-laden simulation, with decreasing fidelity towards the surface. Further study is required to determine to what extent this result is coincidental or significant.

As indicated on the right-hand-side of Fig. 1, the dust-laden profile at 0500 LMT is warmer than the dust-free in the lowest 800 m, an indication of the insulating effect of the dust blanket keeping surface temperature slightly higher in the nocturnal hours. However, in the bulk of the dust layer, a cooling has occurred by 0500 LMT which is substantially larger than in the dust-free case. This is thought to be attributable to the adopted "grey-body" emission of the dust particles, which results in more photons generated in spectral intervals outside the CO_2 absorption bands.

Atmospheric and subsoil temperature profiles in the layers near the interface are shown in Fig. 2, for the dust-free case. The early-morning atmospheric profiles exhibit diffusionlike heat transport characteristics, due to the dual action of strong-line radiative and molecular-conductive transfer. An "effective radiative-conductive diffusivity" may be estimated by L^2/τ where L and τ are the characteristic length and time scales of the Diffusion" process. This diffusivity is found to be $\sim 2 \times 10^5$ cm^2 sec^{-1}, on the basis of data represented in Fig. 2. This compares well with Gierasch and Goody's (1968) scaling estimate of 10^5 cm^2 sec^{-1}, and is similar in order-of-magnitude to a free-convective eddy diffusivity under mildly-unstable conditions. It also tends to corroborate Goody and Belton's (1967) estimate that the time for relaxation of thermal perturbations by radiation and mild turbulent convection should be comparable for a perturbation length scale of hundreds of meters.

Each of the various heat flux components acting at the soil-atmosphere interface are shown as a function of the time of the day in Fig. 3. The limited computational resolution in the atmospheric surface boundary layer cannot produce temperature gradients steep enough to model realistically the removal of heat from the interface by atmospheric conduction. However, the NET curve in Fig. 3 indicates the energy surplus or deficit available to change the interface

temperature. Short-term oscillations of decreasing amplitude evident in the first two hours of the simulation represent the dissipative smoothing of inconsistencies in the arbitrary initial temperature distribution in the interface and subsoil layers.

The fact that the model does not reproduce the initial flux values after 24 hours can be traced to at least two possible causes. One cause related to limited computational resolution has been discussed in the previous paragraph. A second possible cause is that the initial atmospheric temperature profile may not be representative of the local time and season relevant to the IRIS measurement on which the inverted sounding is based. The preliminary Mariner 9 sounding which we utilize was based on an inversion method which assumes a dust-free atmosphere.

Molecular-conductive heat flux in the soil material is a significant fraction of the net flux available for temperature changes, at all times during the 24 hr simulated period. The conductive flux reaches a maximum about 1.5 hours before local noon, in agreement with measurements under comparable terrestrial physical settings (Sellers, 1965).

Atmospheric counter-radiation varies little over the diurnal cycle. Since the concentration distribution of radiatively-active gases remains constant in the model, any temporal variation in counter-radiation can be traced directly

to variations in the temperature distribution, for the dust-free case. The addition of a simulated dust layer results in an increased counter-radiation for all times of the day, as evidenced in Fig. 3. This phenomenon accounts for a higher minimum morning temperature of 198K for the dust-laden case, as compared with 193K for the dust-free simulation.

Height-time cross-sections of the temperature field between 4 and 18 km of altitude are shown in Fig. 4a, b. Because the pattern between the surface and 4 km is nearly unchanged by the presence of dust, it is not shown here. The region between 4 and 18 km is drastically modified by the dust layer during the daylight hours. This regime responds to direct solar heating and to a lesser extent, to interface-temperature variation. The dust-laden layers above 7 km develop a nearly isothermal stratification in the afternoon hours, in agreement with recent Mariner 9 observations. Detailed interpretation of additional features in Fig. 4 will be presented in the near future.

Acknowledgements. The work reported in this note was partially supported under NASA grant NGR 26-006-042. The cooperation of Drs. Hanel and Pearl of the Goddard Space Flight Center in providing Mariner 9 preliminary data is gratefully acknowledged.

REFERENCES

Drayson, S., 1972: Atmospheric radiative transfer by carbon dioxide. Preprints, Conference on Atmospheric Radiation, Fort Collins, Colo., Amer. Meteor. Soc., 77-79.

Gierasch, P., 1971: Dissipation in atmospheres: The thermal structure of the Martian lower atmosphere with and without viscous dissipation. J. Atmos. Sci., 28, 315-324.

Gierasch, P., and R. Goody, 1967: An approximate calculation of radiative heating and radiative equilibrium in the Martian atmosphere. Planet. Space Sci., 15, 1465-1477.

_____, 1968: A study of the thermal and dynamical structure of the Martian lower atmosphere. Planet. Space Sci., 16, 615-646.

_____, 1972: The effect of dust on the temperature of the Martian atmosphere. J. Atmos. Sci., 29, 400-402.

Goody, R., and M. Belton, 1967: Radiative relaxation times for Mars: a discussion of Martian atmospheric dynamics. Planet. Space Sci., 15, 247-256.

Hanel, R., et alii, 1972: Infrared spectroscopy experiment. JPL Tech. Rept. 32-1550, Pasadena, Calif., 27-33.

Jet Propulsion Laboratory, 1968: Mars scientific model. Vol. 1. JPL Document No. 606-1.

Kuo, H.L., 1968: The thermal interaction between the atmosphere and the earth and propagation of diurnal temperature waves. J. Atmos. Sci., 25, 682-706.

Pallmann, A.J., 1968: Radiative heating and cooling functions for the lower Martian atmosphere under the condition of local thermodynamic equilibrium (LTE). Contractor Rept. NASA CR-1044.

Pallmann, A.J., and W. Dannevik, 1972: Transient variation of Martian ground-atmosphere thermal boundary layer structure. Preprints, Conference on Atmospheric Radiation, Fort Collins, Colo., Amer. Meteor. Soc., 288-291.

Prabhakara, C., and J. Hogan, Jr., 1965: Ozone and carbon dioxide heating in the Martian atmosphere. J. Atmos. Sci., 22, 97-109.

Robinson, N. (ed), 1966: Solar Radiation. Amsterdam, Elsevier Publishing Co., 347 pp.

Schlichting, H., 1968: Boundary Layer Theory. New York, McGraw-Hill Book Co., 747 pp.

FIGURE LEGENDS

Fig. 1a. Modeled vertical temperature profiles at 0500 and 1600 local Martian time (LMT), for the dust-free (solid line) and dust-laden (dashed line) conditions. Also shown is the initial (1900 LMT) profile obtained from inversion (Hanel, et al., 1972) of Mariner 9 IRIS measurements by assuming a dust-free atmosphere.

Fig. 1b. Profiles of the difference $\Delta T = T_c - T_d$ in temperature between the dust-free (subscript:c) and dust-laden (subscript:d) simulations, at 0500 and 1600 LMT.

All results based on following simulation parameters: latitude $\phi = -38^{\circ}$, solar declination $\delta = -23^{\circ}$ (Southern hemisphere summer), surface albedo $\alpha_s = 0.25$, surface infrared emissivity $\varepsilon = 1.0$, soil thermal conductivity $k_s = 2.3 \times 10^5$ erg cm^{-1} sec^{-1} K^{-1} (low-porosity silica), and CO_2-gas thermal conductivity $k' = 1.33 \times 10^3$ erg cm^{-1} sec^{-1} K^{-1}.

Fig. 2. Vertical temperature distributions in the subsoil and lower atmospheric layers for selected hours of the Martian day, from the dust-free simulation. For environmental parameters used, see Fig. 1.

Fig. 3. Diurnal history of the various component heat fluxes at the soil-atmosphere interface. EMIS represents the flux of long-wave radiation emitted by the surface, SCON the molecular-conductive heat flux in the soil material, SOL the absorbed insolation, ACR the absorbed flux of atmospheric counter-radiation, and NET the algebraic sum of all component heat fluxes. Solid lines depict results for dust-free conditions, while the dashed lines (shown for EMIS, SOL, and ACR only) relate to the simulated dust-laden conditions. Influence of CO_2-gas thermal conduction is of lesser significance at the interface, and curve is not shown.

Fig. 4a,b. Height-time cross-sections of the modeled temperature field (deg. K) between 4 and 18 km for (a) dust-free, and (b) dust-laden conditions. Approximate extremal lines are dashed.

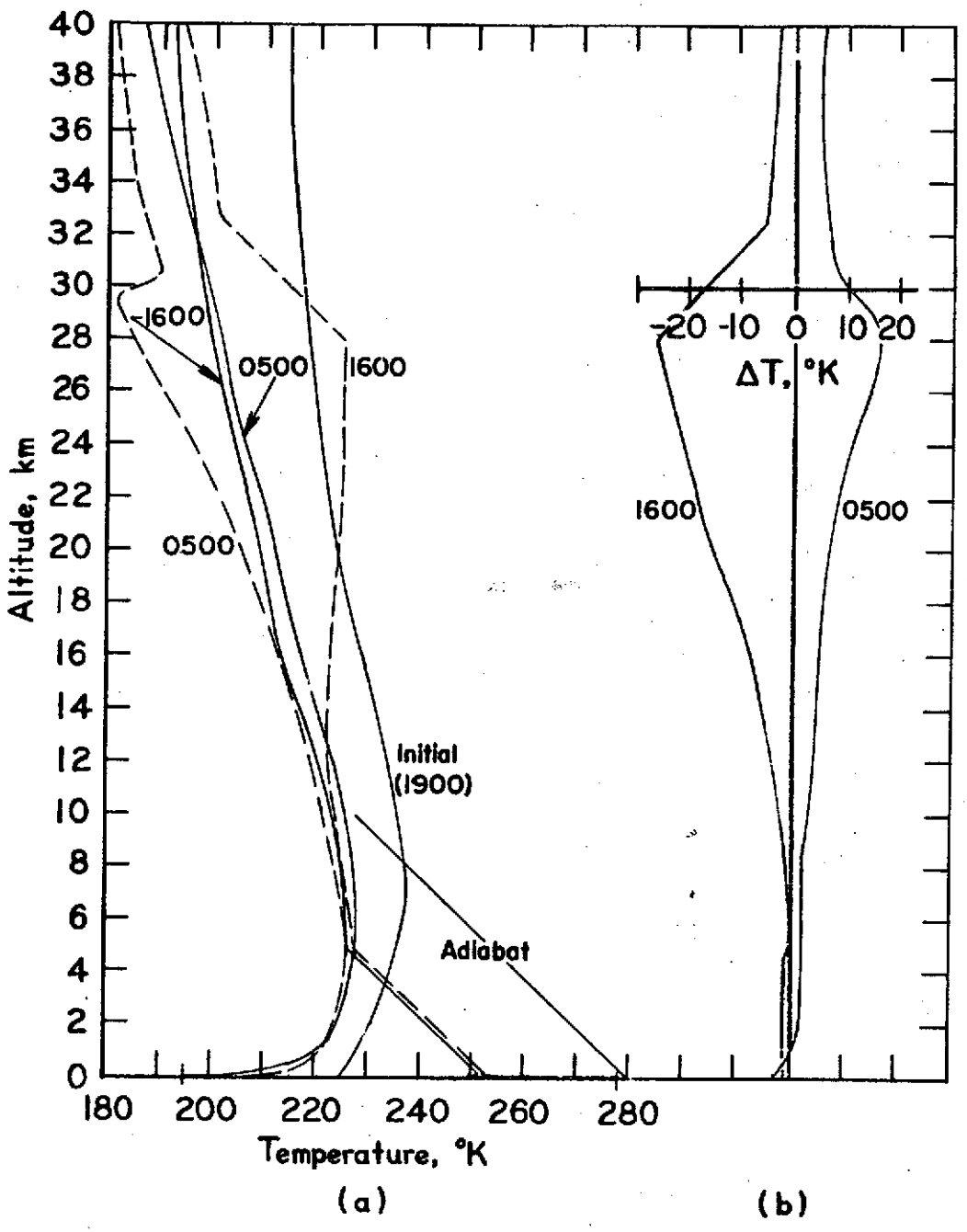
Altitude, km
Temperature, °K
ΔT, °K
1600
0500
1600
0500
Initial
(1900)
Adiabat
1600
0500
(a)
(b)

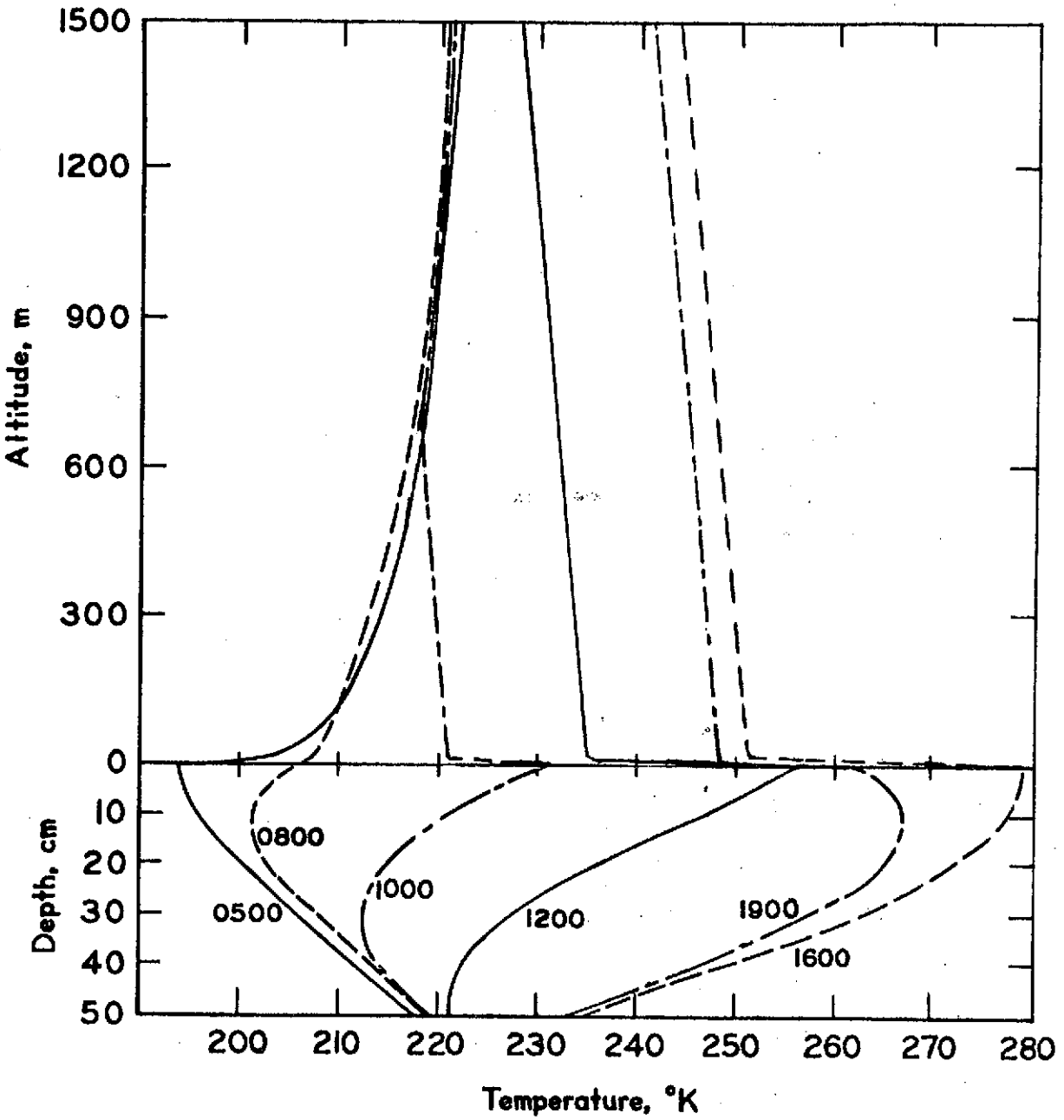
1500
1200
900
600
300
0
Altitude, m
10
20
30
40
50
Depth, cm
0800
1000
0500
1200
1900
1600
200
210
220
230
240
250
260
270
280
Temperature, °K

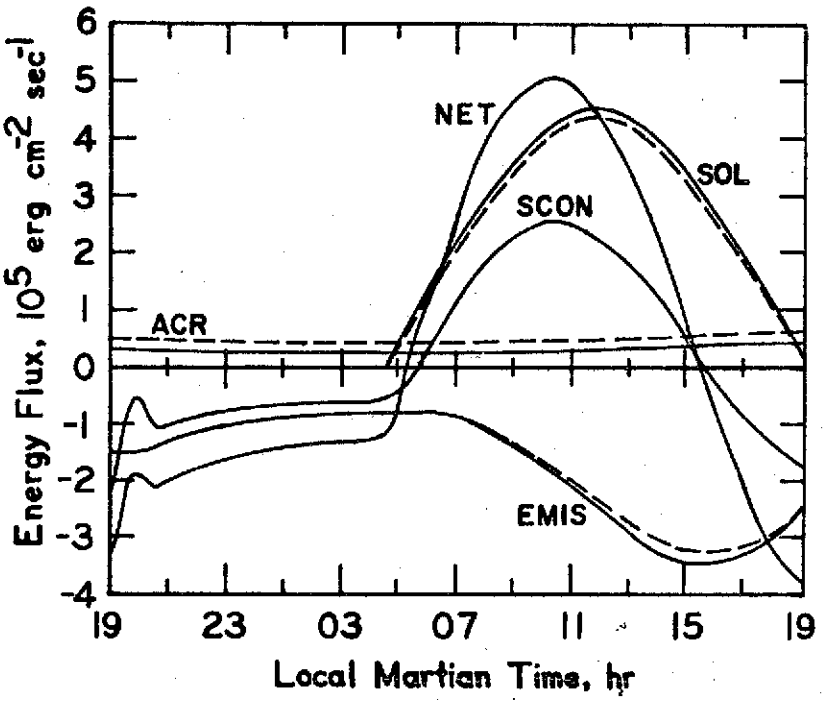
Energy Flux, 10^5 erg cm^{-2} sec^{-1}
6
5
4
3
2
1
0
-1
-2
-3
-4
NET
SOL
SCON
ACR
EMIS
19
23
03
07
11
15
19
Local Martian Time, hr

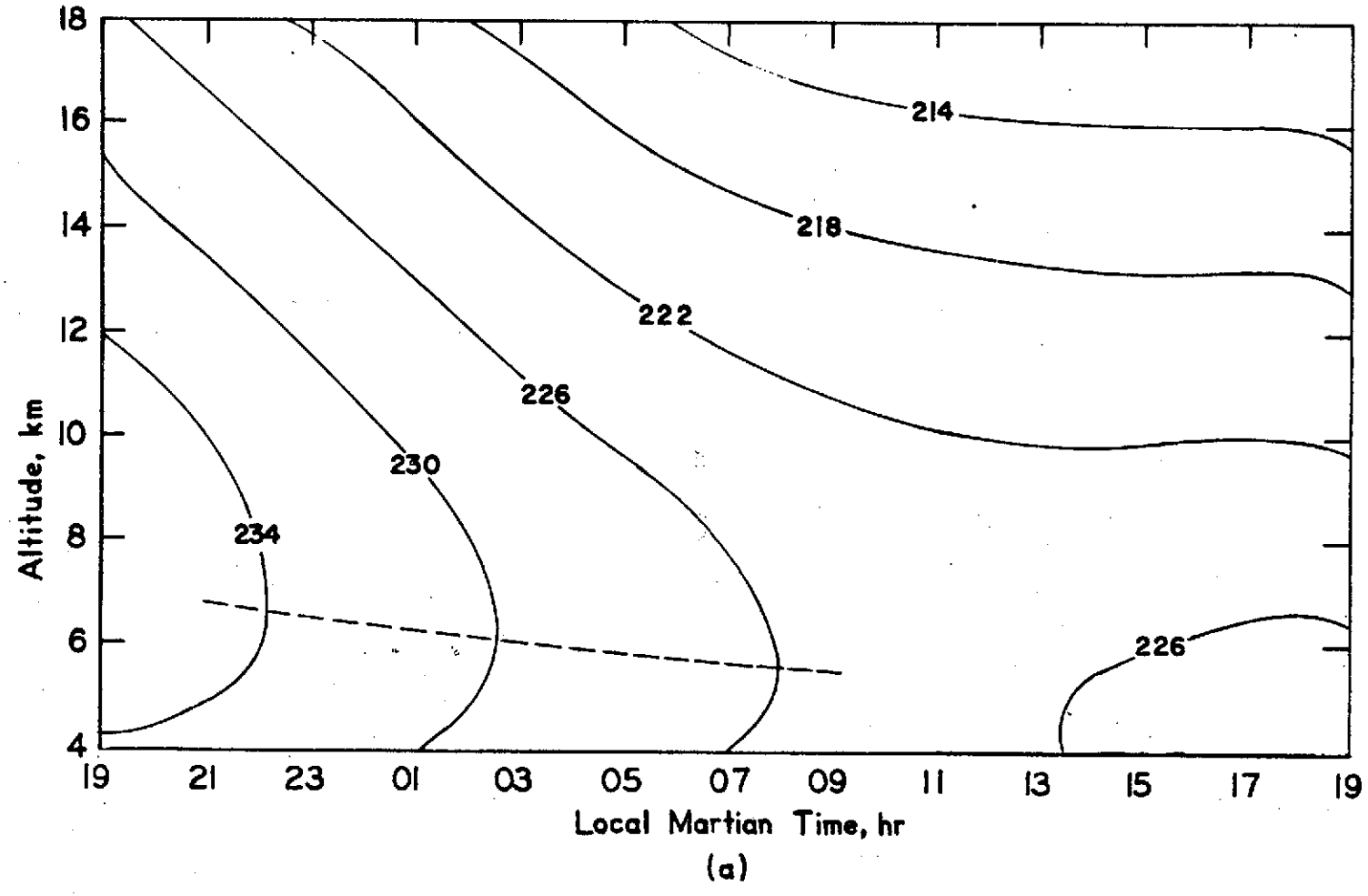
18
16
14
12
10
8
6
4
Altitude, km
214
218
222
226
230
234
226
19
21
23
01
03
05
07
09
11
13
15
17
19
Local Martian Time, hr

(a)

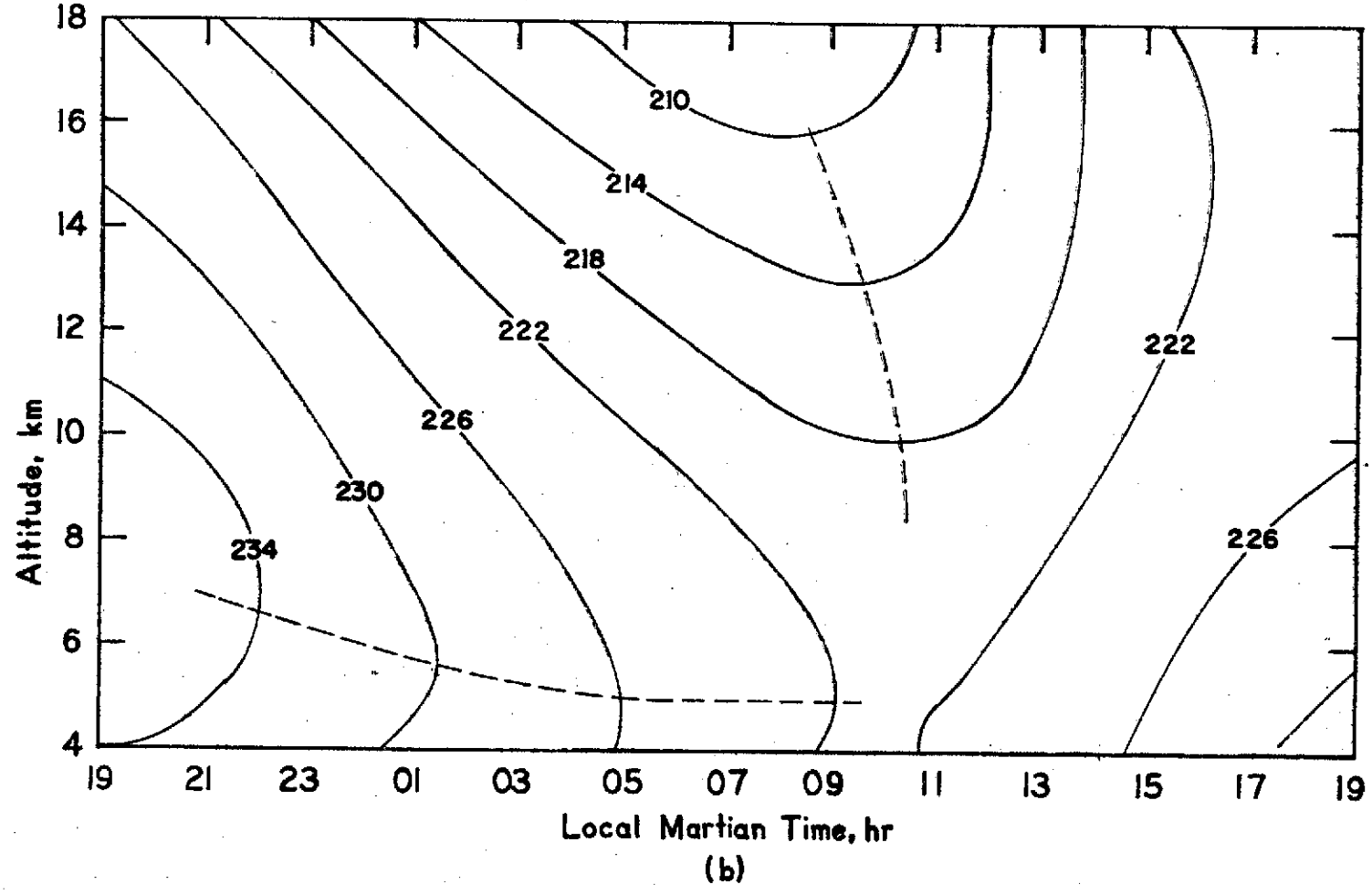
18
16
14
12
10
8
6
4
Altitude, km
210
214
218
222
226
230
234
222
226
19
21
23
01
03
05
07
09
11
13
15
17
19
Local Martian Time, hr

(b)